Iraqi National Journal of Earth Science, Vol. 26, No. 03, 2026 (237-252)

Iraqi National Journal of Earth Science

www.earth.uomosul.edu.iq

Rock Slopes Stability Analysis along the Road of (Al-Rabban Hormizd) Monastery in Alqosh Anticline, Northern Iraq

Nawal M. Al Abdullah [1*], Mohammed R. Abood[2], Amaar J. Mohammed [3]

nawal.muhammad@st.tu.edu.iq mrabood@tu.edu.iq geoamaar1977@edu.tu.iq

[1] *Nineveh Education Directorate, Country, Iraq.*
[2] *Department of Applied Geology, College of Science, University of Tikrit, Tikrit, Iraq.*
[3] *Department of Applied Geology, College of Science, University of Tikrit, Tikrit, Iraq.*

Received: 24 March 2025 Received in revised form: 06 May 2025 Accepted: 09 June 2025
Available online: 01 July 2026

Abstract

The aims of the current study include slope stability analysis conducted by kinematic analysis and Slope Mass Rating (SMR) at six selected stations on the road to (Al-Rabban Hormizd) Monastery located at Alqosh anticline, northern Iraq. The current study shows that station (1) has the possibility of two cases of direct toppling by intersection (J1) with both bedding plane (So) and (J3), both of which are stable conditions. Station (2) shows two possible cases: planner sliding on (J2), which is a bad and unstable condition. The second possible case is direct toppling from the intersection of (J1) with (J3), which is a good and stable condition. Station (3) shows two possible cases; the first is the planner sliding of (J2) with an (SMR) value of (23), so it is bad and unstable. The second is the wedge sliding from the intersection of (J2 with J3), which is a good and stable. At station (4), three possible failure cases appeared. The first is planner sliding on (J1), which is bad and unstable. The second possible case is the wedge sliding from the intersection of (J1) with both (J2 and J3), and in both cases the (SMR) value is (65), so they are both good and stable cases. The third possible case is the direct toppling from the intersection of (J2 with J3), which is normal and partially stable. Station (5) shows two cases; first is a wedge sliding from the intersection (J1 with J2), which is good and stable; second is a flexural toppling on (J3), which is normal and partially stable. Station (6) shows two cases; first is a planer sliding on (J3) with an (SMR) value of (13), which is very bad and completely unstable, and requires support by (Re-excavation Walls); second possible case is a wedge sliding from the intersection (J3) with both (J1 and J2), both are normal and partially stable.

Keywords:

Rabban Hormizd, Kinematic analysis, support types.

DOI: 10.33899/injes.v26i3.60933, ©Authors, 2026, College of Science, University of Mosul.

==========

1. Introduction

The slope stability analysis has received wide attention at present due to its great importance, as various investigations are conducted to ensure stable and safe slopes regardless of their steepness. The field of slope stability includes the evaluation and ensuring stability of slopes in various types of engineering facilities like infrastructure projects such as tunnels, roads, and bridges (Duncan, 2000; Al-Jawadi, 2021), geotechnical engineering and mining works (Hoek and Bray, 1981), dam projects of all kinds (Fell et al., 2014; Al-Habity et al., 2025). Moreover, in the field of the environment (Rowe, 2001), in anticipating the risks of landslides and earthquakes and developing their strategies (Iverson, 2000), as well as in determining the best methods for rehabilitating lands that may be damaged by environmental disasters due to slopes, whether soil or rocky (Clague and Steed, 2012), and many others.

Slopes may be unstable for various reasons; some are natural, and some are caused by human activities. Slope instability may occur due to earthquake activities, geomorphological features, or weathering factors (Hoek and Bray, 1981). They may also fail due to excavation or undermining from below, or due to the gradual disintegration of the soil structure. Landslides may occur slowly or suddenly with or without clear provocation (Bromhead, 1992). The main objectives of slope stability analysis are finding the most vulnerable areas, investigating potential forms of failure, and

predicting the stability or failure of those slopes, whatever their type. In addition, the slope stability investigation aims to design the optimal slopes in terms of safety and reliability and design possible remedial measures (Salunkhe et al., 2017). Most of the proposed methods for slope stability analysis share a set of obstacles, which are related to their scope of application or their reliance on data that is difficult to obtain. Therefore, assessing the stability status of any slope is a multidimensional and multifactorial problem (Ullah et al., 2020). With the recent developments witnessed by the world in all fields and modern method technologies for rock and soil testing and stability analysis, artificial intelligence algorithms and computer technologies, it has become easy to implement any of the methods in a safer way for the slope, faster and more economically.

The present study used the kinematic analysis due to the dominance of the structural situation on the nature of the slopes, geomorphological features, and failure occurring in the region. The Slope Mass Rating (SMR) system is also used to analyze slope stability, which is one of the geomechanical classifications as a preliminary assessment of slope stability, as it provides some simple rules about the instability conditions and the required support measures. The extensive use of this system in different parts of the world has led to the accumulation of extensive experiences that confirmed the usefulness of the SMR classification and its acceptance and recognition by the international community in the scientific and technological fields (Romana et al., 2015).

Rock slopes, in most cases of road cuts, especially in mountainous areas, are exposed to instability due to variations in rock mass conditions and external factors like environmental influences such as seismic activities, weather conditions, and heavy rains (Pantelidis, 2009). The road to the Monastery of (Al-Rabban Hormizd), which appears suspended in the middle of the Alqosh Mountains (Fig. 1), is crowded with visitors during religious holidays. It is also a summer destination and can be rehabilitated in the future by establishing several engineering projects. The road cuts have led to the creation of very rugged slopes in this area. Sissakian et al. (2016) classified the current study area as one of the areas exposed to continuous landslides due to the presence of previous landslides. These reasons led to conducting the current study.

Fig. 1: Location of (Al-Rabban Hormizd) Monastery. Note that the monastery is located in the middle of the mountain.

The Monastery (Al-Rabban Hormizd) road is located in the southern limb of the Alqosh anticline between longitudes (43°6'18.90" E - 43°7'39.78" E) and latitudes (36°45'2.63" N - 36°44'27.34" N). Alqosh is located between Dohuk and Mosul cities, about (45) km away from each. Alqosh anticline is a double-plunging asymmetrical anticline, whose southern limb is more inclined than the northern limb. Its axis extends east-west. The length is (20) km, whereas the width is (6.5) km. Tectonically, it is located in the Unstable Shelf of the Arabian Plate within the High-Folded Zone of the Foreland Basin parallel to the Taurus extension (Jassim and Goff, 2006), (Figs. 2 and 3).

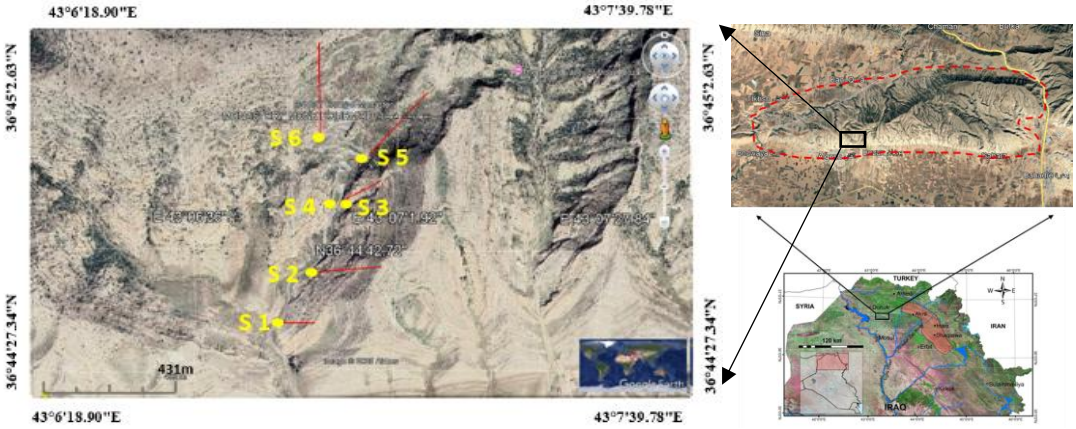

Fig. 2: Location map of the study area.

Fig. 3: Location of stations (a) the stations before the Monastery Gate taken from the top of the second station, (b) the stations after the gate taken from the top of the monastery terraces.

Stratigraphically, four geological formations are exposed in the study area: (1) Gercus Formation (Middle Eocene), which is exposed only at the east of the fold and consists essentially of reddish clastic rock sequences for transitional continental environment; (2) Pila Spi Formation (Middle-Late Eocene), which consists of sequences of well thickly bedded to massive dolostone, dolomitic limestone and limestone representing a shallow coastal - lagoon environment; (3) Fatha Formation (Middle Miocene), which consists of periodic sequence of limestone and marly limestone for a lagoon environment; and (4) Injana Formation (Late Miocene), which consists of alternating sandstone, claystone and siltstone representing diverse depositional environments from shallow coastal to continental. All stations are located on the Pila Spi Formation, which covers most of the study areas.

Geomorphologically, based on satellite images and field trips, the following features are found in the area:

a) Anticlinal Ridges: well-bedded limestone belonging to the Pila Spi Formation.

b) Alluvial fans: they appear in some parts of the fold in areas with steep inclination, especially in the southern limb.

c) Valleys and drainage systems: primary and secondary drainage patterns for a specific area, regardless of whether there is a permanent watercourse or not.

d) Flat Iron topography: appears clearly due to the fine stratification of Pila Spi limestone beds.

e) Mass movement: represented by landslides, rock falls, rolling, toppling, and debris flow.

f) Questa: It consists of inclined rock beds forming two contrasting slopes: a gentle dip slope that follows the bedding inclination, and a steep escarpment slope on the opposite side, developed as a result of differential erosion.

g) Caves: The study area is characterized by a large number of caves with various scales on both fold limbs.

h) Stratification Ribbons: These are produced due to differential erosion and weathering at the stratification levels.

The current study aims to predict potential failures of rock slopes in the study area using kinematic analysis by the DIPs v6.008 package (Rocscience, 2015). This is due to the presence of extremely rugged rock slopes, where frequent rockfalls and landslides occur. Failure is related to the structural condition and the presence of discontinuities that contribute to failure. Another aim is to evaluate the stability of predicted failures using the Slope Mass Rating (SMR) by the SMR Tool-v205 software (Riquelme et al., 2014) due to its accuracy, reliability, and acceptance by the international community (Romana et al., 2015).

2. Materials and Methodology

The comprehensive geological survey of the study area by fieldwork (lasting from 8-15 July 2024) was conducted to identify, select, and evaluate appropriate stations. Slope types are determined in the field following Hock and Bray (1981) to sliding (plane, wedge), toppling (flexural, direct), and rock fall. The geotechnical analysis measurements include the slope attitude (direction and inclination) using a geological compass (Silva). Also, the fieldwork includes measuring the attitude of discontinuities represented by the bedding planes and joints (dip direction/dip amount) and recording the thickness of the beds (minimum and maximum thickness) and the joint spacing (minimum and maximum), persistence (discontinuity length), aperture, roughness, infilling materials, and weathering. Describing the rocks as stated by the General Geological Group of the Engineering Group of the Geological Society of London (Anon, 1972; 1977) is implemented. Then, identifying the history of rockfalls, climate, water infiltration, rockfall sizes, and measuring sliding friction angle using Tilt's method (Bruce et al., 1989) at each station. Lastly, samples of intact rocks from places not exposed to distortion are taken for laboratory analysis; these samples are free from cavities, cracks, and veins, documenting all of these with photographs.

Laboratory work includes preparation of rock samples as regular and conducting a point load test (Broch and Franklin, 1972) as (ISRM, 1985). The office work includes performing mathematical calculations to find the values of Unconfined Compressive Strength (UCS), volumetric joint (Jv), Rock Quality Designation (RQD), spacing average and (RMRb), then (DIPs v6.008) software is utilized for kinematic analysis to identify possible failure cases, and (SMR Tool-v205) package to evaluate the stability of those cases.

A. Rocky slopes

According to Hock and Bray (1981), landslides on rock slopes are divided into:

a) Sliding: It expresses the sliding of rock masses on a surface. Its types are plane, wedge, and rotational sliding.

b) Toppling: It is the overturning of the rock mass around a pivot point, represented by flexural and direct toppling.

c) Rockfall: The free fall of rock pieces down steep or vertical slopes.

d) Rolling: It is the rotation of the separated rock mass around itself down the slope.

Kinematic analysis is used to determine potential structural failure mechanisms by the stereographic projection technique of both slopes and discontinuities as poles and great circles with sliding friction angles (Al Sumaidaie et al., 2024). The probability of plane sliding and flexural toppling is inferred from the occurrence of discontinuity poles within the potential slip zone. The probability of wedge sliding and direct toppling is also inferred from the occurrence of the intersection point of two discontinuity planes within the potential slip zone (Markland, 1972).

B. Rock Mass Rating System (RMR)

It is an interconnected system of intact rock properties with discontinuities, which includes basic parameters: unconfined compressive strength, rock quality index (RQD), spacing, discontinuity conditions, groundwater, and finally the orientation of discontinuities according to Bieniawski (1973, 1989).

C. Unconfined compressive strength (UCS)

It is a geotechnical property that is often cited in rock mechanics. It is measured in several ways; the easiest (used in the current study) is the Point Load Test (Broch and Franklin, 1972). It is an easy-

to-implement method that requires little effort to prepare the sample (Gunsallus and Kulhawy, 1984). Samples of different geometric shapes can be used, cylindrical, regular, or irregular, and each of these geometries has dimensions with specific proportions (Fig. 4). The equations used are:

$$A = D*W \quad \text{……(1)}$$

where: A: Cross-sectional area of the samples (mm^2); D: Thickness of the samples (mm); W: Width of the samples (mm).

$$D_e = \sqrt{(4A)\backslash\pi} \quad \text{……(2)}$$

where: D_e: Diameter of the samples (mm).

$$I_s = P\backslash D_e^2 \quad \text{……...(3)}$$

$$f = (D_e\backslash 50)^{0.45} \quad \text{…...……...(4)}$$

$$I_{s(50)} = I_s * f \quad \text{……...…(5)}$$

$$UCS = 21*I_{s(50)} \quad \text{…… …..(6)}$$

where: I_s: Point load strength index (MPa); P: Strength at failure of the sample (KN); f: Correction factor; $I_{s(50)}$: Corrected point load strength index of the sample at diameter (50 mm); UCS: Unconfined compressive strength (MPa) according to Rusnak and Mark (2000).

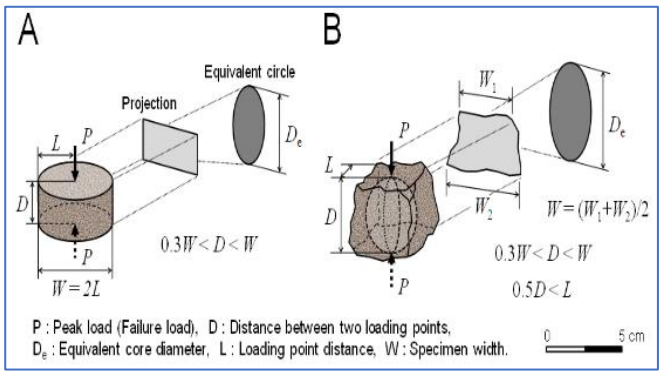

Fig. 4: Ratios between geometric dimensions of samples. (A) for cylindrical samples, (B) for regular and irregular samples (From Kohno and Maeda, 2018).

D. Rock Quality Designation (RQD)

It is a method for describing rock mass developed by Deere et al. 1966); it is measured from the core, but in the absence of the core, when the traces of discontinuities are evident in the outcrop. Palmström (1982) proposed a method for estimating RQD based on the number of discontinuities per unit volume (used in the current study) by finding volumetric joint count (J_v), which represents the sum of the number of joints per unit length for all discontinuities in the rock exposure:

$$J_v = \sum_{i=1}^{J} \frac{1}{Si} \quad \text{……...(7)}$$

$$RQD = 115-3.3\ J_v \quad \text{…… ….(8)}$$

where: J_v: Volumetric joint count; Si: Joint spacing ratio; i: Joint sets; J: Total number of joint sets excluding random joint aggregates; RQD: Rock quality index.

Depending on (J_v), the spacing between discontinuities can be found by:

$$A_f = J_v\backslash n \quad \text{……(9)}$$

$$Si = 1\backslash A_f \quad \text{…… …...(10)}$$

where: A_f: the average of (J_v), n: number of discontinuities, and (Si): spacing between discontinuities (It is also symbolized as DS in other references).

E. Slope Mass Rating System (SMR)

This system was developed by Romana (1985). It is a geomechanical system that was basically derived from the classification of Bieniawski (1973). It includes five classes, to which six support proposals were added later (Fig. 5). The value of SMR is expressed by the equation:

$$SMR = RMR_{basic} + (F_1 * F_2 * F_3) + F_4 \quad \text{……...(11)}$$

where: $F1$, $F2$, $F3$, $F4$ are factors (will be explained later); RMR_{basic} represents the first five parameters of the rock mass rating system (RMR) based on the latest modification of Bieniawski (1989) as in the equation:

$$RMR_{basic} = UCS+RQD+DS+DC+GW \quad \text{……...(12)}$$

where: UCS refers to the unconfined compressive strength; RQD expresses the rock quality designation index; DS is the spacing between discontinuities (it is symbolized Si in equations 7 and10) according to Palmström (1982); DC is the five discontinuity conditions; GW is the groundwater condition.

Instead of the orientation of discontinuities in Bieniawski (1989), the correction factors proposed by Romana (1993) and Romana et al. (2003) are used to create the (SMR) system, represented by F_1, F_2, F_3, and F_4. Where (F_1) is the difference between

the dip direction of joints (αj) and the dip direction of the slope (α_s). This factor is measured by:

$$F_1 = (1-\sin|\alpha_j-\alpha_s|)^2 \text{……..(13)}$$

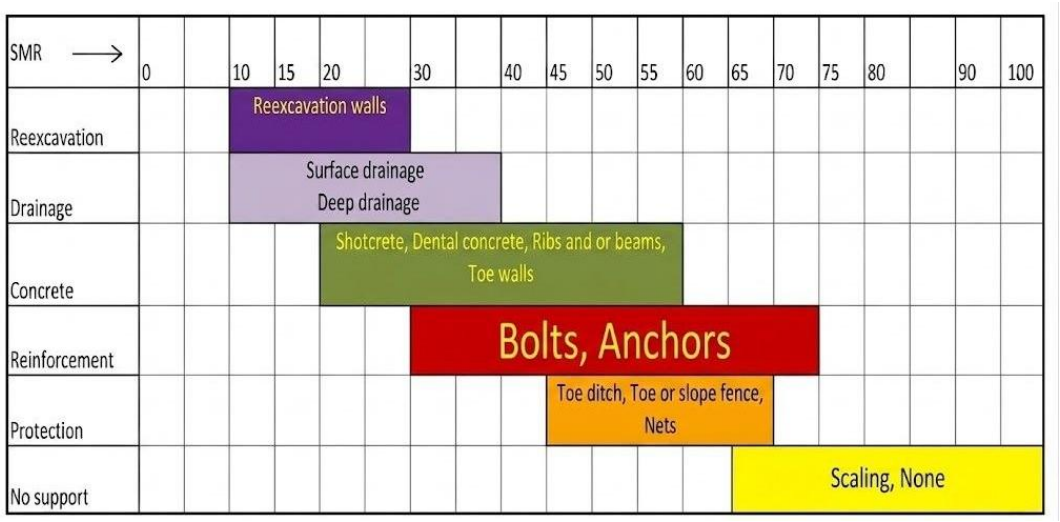

Fig. 5. Six types of support proposed by Romana et al. (2015) from Romana (1985) according to (SMR) values.

(F_2) is an indicator of the probability of shear strength of the joint; its value ranges between (0.15 - 1.0), can be found from:

$$F_2 = \tan^2\beta_j \text{……..(14)}$$

where: β_j depends on the dip angle of the joint.

(F_3) is the relationship between the dip of the slope (βs) and the dip of discontinuities (βj), ranges between (0-60).

The fourth factor (F_4) depends on the excavation; its value ranges between (-8) for a slope that cuts poorly to (+15) for a natural slope.

The slope stability analyses are distributed at six stations in the study area, which are chosen based on the occurrence or possibility of failure; two stations are before the gate of the monastery and four stations after the gate of the monastery. These slopes appear as a result of the mechanical cutting of the road. To find the Unconfined Compressive Strength (UCS), the samples are cut and prepared in a regular geometric shape to conduct the Point Load Test for easy sample preparation. Table 1 shows the results of the compressive strength test.

3. Results and Discussion

Table 1: Results of unconfined compressive strength (UCS) by point load test, (L) refers to the distance between the edge of the specimen and the load point, and (S) refers to the stations.

stations	L (mm)	D (mm)	W (mm)	A(mm^2)	P (KN)	De (mm)	*f*	Is (MPa)	$Is_{(50)}$ (MPa)	UCS (MPa)
s1	41	50	60	3000	18.13	61.8195	1.1002	4.744	5.219	**109.60**
s2	40	46	63	2898	6.51	60.759	1.09	1.763	1.921	**40.355**
s3	40	47	62	2914	30.07	60.927	1.093	8.101	8.853	**185.913**
s4	40	50	56	2800	0.64	59.723	1.0832	0.179	0.1943	**4.08**
s5	39	43	62	2666	3.34	58.276	1.0714	0.9834	1.0536	**22.126**
s6	40	47	60	2820	0.38	59.936	1.085	0.1058	0.1148	**2.410**

Table (1) shows that the (UCS) values vary between (185.913 MPa) as the highest value and (2.410 MPa) as the lowest value. UCS is between (very strong) and (very weak) according to Anon (1977). High values of (UCS) lead to an increase in the value of (RMR_b), thus causing an increase in the stability of slopes.

Mathematical calculations are carried out to determine the values of (RMR_{basic}) parameters, where the values of (J_v) are first obtained; then, the spacing (DS) and (RQD) are determined based on

the (J_v) values. The values are assigned ratings as explained previously. Finally, the (RMR_{basic}) values are calculated using equation (12).

Table (2) shows discontinuity conditions that were observed in the field. It is very important in rock mass behavior and has high rates (Bieniawski, 1989). If the fracture density is normal and if the fractures are neither rare nor severe, the rock mass is classified based on discontinuity properties. The strength of the rock mass is reduced due to the inefficiency of the discontinuity properties represented by roughness, aperture, persistence, spacing, attitude, and normal stress (Al-Jawadi et al., 2023). Anyway, the rough joint surface reduces failure; on the other hand, the large aperture with soft infilling increases the possibility of failure.

Table 2: Conditions of discontinuities observed in the field with their rates, where So is bedding plane, and J is joint sets.

stations	C.D	Discontinuities	Thickness\m		Condition of discontinuities				
			Min.	Max.	persistence \m	Aperture\m	roughness	infilling	weathering
S1	14	S_o	0.05	1.5	<20	--	slightly	--	slightly
		J_1	0.3	1.5	<20	0.05	slightly	hard f.	slightly
		J_2	0.07	0.5	3	0.02	slightly	hard f.	slightly
		J_3	0.1	1.0	<20	--	slightly	hard f.	slightly
S2	14	S_o	0.5	3	<20	--	slightly	--	slightly
		J_1	0.1	1	3	0.01	slightly	hard f.	slightly
		J_2	0.05	2	<20	0.1	slightly	hard f.	slightly
		J_3	0.1	1	3	--	slightly	hard f.	slightly
S3	12	S_o	0.2	2	<20	--	slightly	--	slightly
		J_1	0.2	0.9	<20	0.03	slightly	hard f.	slightly
		J_2	0.15	0.7	<20	0.01	slightly	hard f.	slightly
		J_3	0.2	1.5	<20	0.01	slightly	hard f.	slightly
S4	16	S_o	0.3	2	<20	--	slightly-rough	--	slightly-moderate
		J_1	0.05	1	6	0.01	slightly-rough	--	slightly-moderate
		J_2	0.15	1.1	2	0.03	slightly-rough	--	slightly-moderate
		J_3	0.2	1.3	0.9	0.01	slightly-rough	--	slightly-moderate
S5	13	S_o	0.1	1	<20	--	slightly	--	slightly
		J_1	0.2	1.5	<20	0.02	slightly	--	slightly
		J_2	0.05	1	<20	0.01	slightly	hard f.	slightly
		J_3	0.2	1.5	14	0.01	slightly	hard f.	slightly
S6	15	S_o	0.02	1.5	<20	--	slightly - smooth	--	slightly
		J_1	0.15	0.9	10	0.04	slightly-smooth	hard f.	slightly
		J_2	0.2	0.5	6	0.02	slightly-smooth	--	slightly
		J_3	0.3	1.5	3	0.05	slightly-smooth	--	slightly

Table (3) shows the results of (RMR_{basic}) with its parameters and sliding friction angle for discontinuities at each station. The values of (RMR_{basic}) range between (63-75), indicating that the rock mass is good in terms of geotechnical and engineering properties. It is also worth noting that the high values of the sliding friction angle increase the stability of the slopes, in contrast to the low values, which reduce slope stability.

Table 3: Results of (RMRbasic), (DS), (Jv), (RQD) with their respective ratios, groundwater, discontinuity conditions, and sliding friction angle (ϕ).

Stations	(Dip direction\ Dip amount)					Jv	DS m	rate	RQD	rate	UCS MPa	rate	G.W Rts.	C.D Rts.	RMRb	ϕ
	Slope	Bedding	J_1	J_2	J_3											
S1	291\75	141\44	048\66	215\42	098\24	7.71	0.519	10	89.6	17	109.60	15	11	14	67	36°
S2	308\77	197\16	047\71	325\76	060\57	5.18	0.772	15	97.89	20	40.4	15	11	14	75	32°
S3	277\90	187\13	357\19	279\82	036\79	6.23	0.642	15	94.4	20	185.91	15	11	12	73	42°

S4	093\89	165\33	111\84	353\67	010\82	5.66	0.707	15	96.32	20	4.08	12	11	16	74	38˚
S5	218\84	203\26	261\72	314\77	047\66	6.08	0.658	15	94.95	20	22.126	15	11	13	74	36˚
S6	146\77	160\21	286\58	229\67	142\73	7.19	0.556	10	91.27	20	2.410	7	11	15	63	29˚

The discontinuity, slope orientations, and sliding friction angle are entered into the (DIPs v6.008) software (Rocscience, 2015) to conduct a kinetic analysis to determine the probability of failures occurring and determining their directions. This software uses the average slope and discontinuity attitudes to determine probable structurally controlled failure. The results are used to conduct the initial assessment of slope stability with some guidelines for the use of support means based on the SMR values by the SMR (Tool-v205) program. The results of fieldwork are as follows:

The rock-cut slopes consist generally of thick-massive beds of Pila Spi Formation.

Station (1) consists of fine-grained, light brown, and different thicknesses of bedded limestone with veins and chert nodes. Station (2) is composed of light to dark brown limestone, and the lower part of the slope is more steeply inclined than the upper part; there are hanging rock blocks with discontinuities that facilitate failure, and (J_2) has a high aperture. In station (3), the slope has a very high inclination approaching the vertical in most parts; the face exposes beds of dark brown limestone. Station (4) that consists of light to dark brown limestone beds, which are exposed in the face with high deformation. On the other hand, station (5) consists of light brown dolomitic limestone, where the spacing in the upper part seems large. The last station (6), in which dolomitic limestone beds are exposed in the face, is composed of chert veins with a large thickness of more than 7 cm. Stations (3, 4, 5, and 6) have retaining walls at the bottom of the slopes. There are large fallen blocks in stations (5 and 6), some of which led to the destruction of parts of the retaining wall, and due to the difficulty of removing them, due to their large size, they were attached to the retaining wall, in addition to many blocks close to falling due to water penetration into the voids, which poses a great danger to visitors of the site or cars parked in front of it (Figs. 6, 7, 8, 9, 10, and 11).

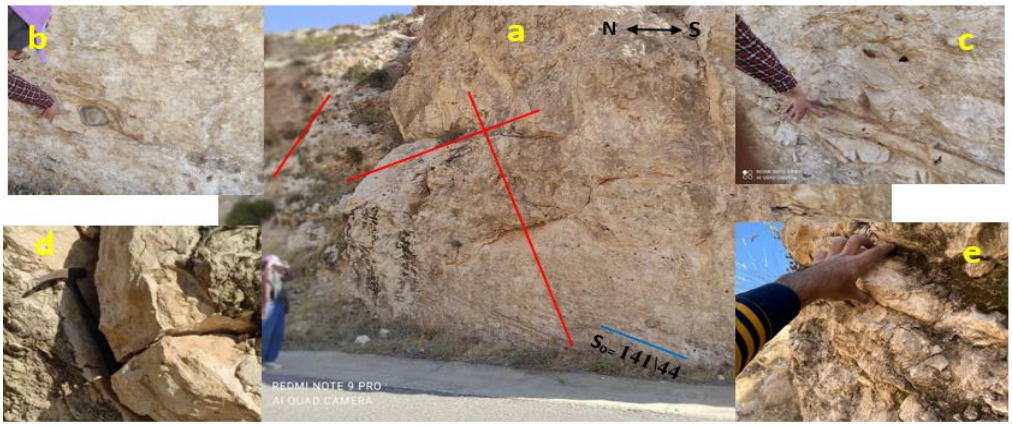

Fig. 6: Station (1): (a) discontinuities in the station, where the red colour indicates the joints and blue for bedding, (b) chert nodes, (c) vein sets, (d) opening between the discontinuities, and (e) different thicknesses of the bedding plane.

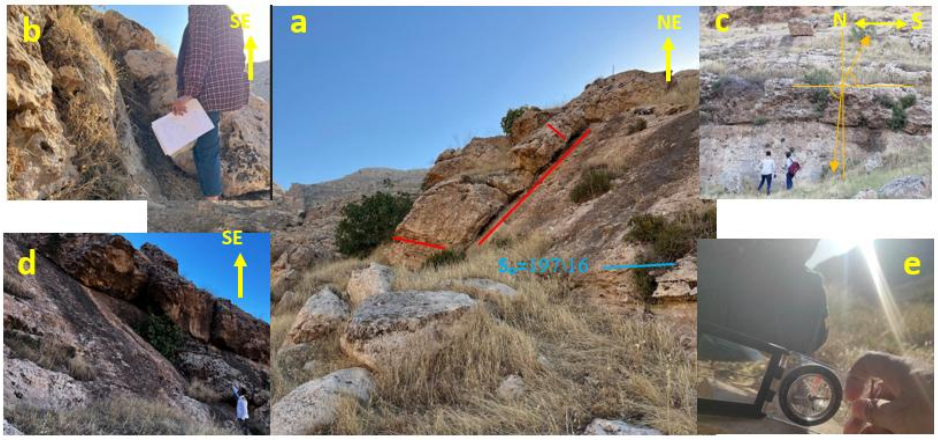

Fig. 7. Station (2): (a) Discontinuities at the station, note how J2 has become a supportive surface for sliding, (b) High aperture of J2, (c) Front view of the station showing the high incline of the lower part of the slope and the upper part appears less inclined, (d) Hanging rock blocks with discontinuities that facilitate failure, and (e) sliding friction angle of the rocks at the station.

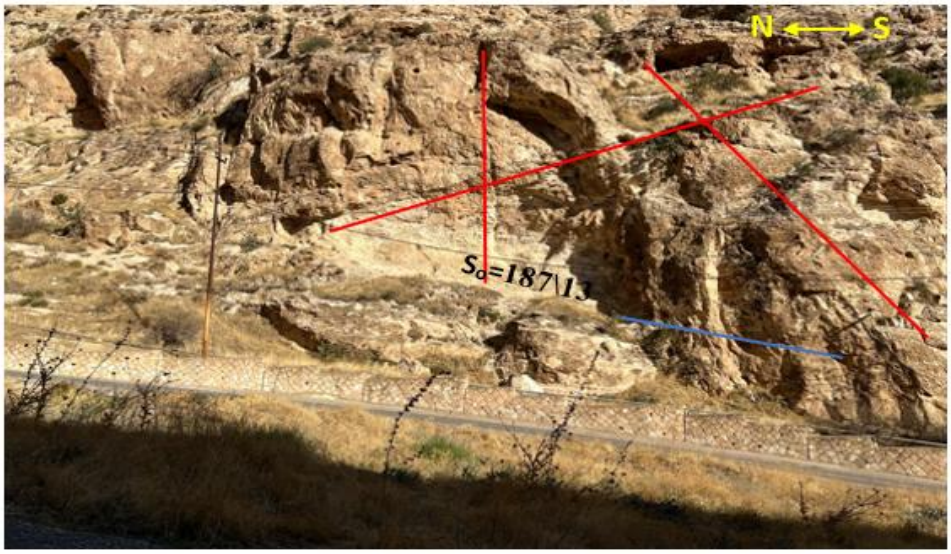

Fig. 8: Station (3): front view of the station showing the discontinuities, note the retaining wall at the bottom of the slope.

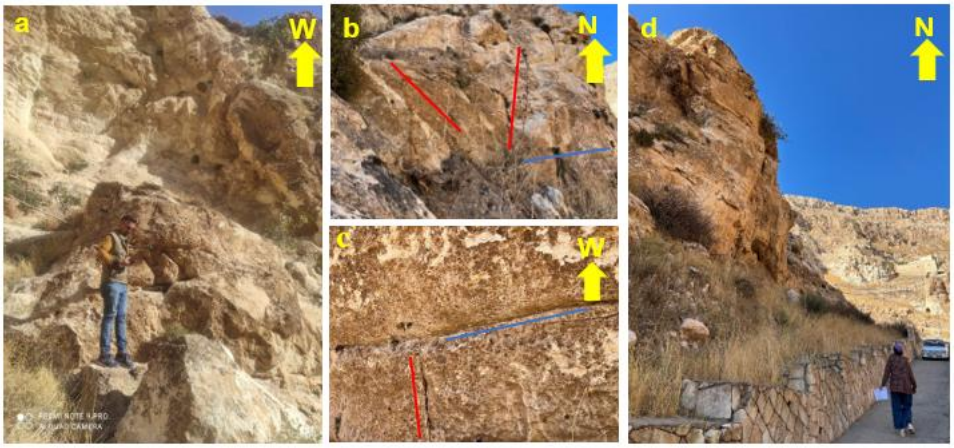

Fig. 9: Station (4): (a) Front view of the station, note the significant deformation of the station, (b and c) Discontinuities, (d) Side view of the station looking north, note the retaining wall at the bottom of the slope.

Fig. 10: Station (5): (a) Front view of the station showing part of the retaining wall destroyed by blocks falling from the top of the station, (b) Discontinuities in the station.

Fig. 11: Station (6), (a) Side view of the station. (b) Part of the station showing part of the retaining wall destroyed by blocks falling from the upper part. (c) The chert veins showing a thickness of 7.0 cm.

Kinematic evaluations of six stations are shown in figures (12, 13, 14, 15, 16, 17) that are projected using (DIPs v6.008) software, exhibiting that:

There is a possibility of direct toppling failure at station (1) resulting from the intersection of (J_1 with S_o) in direction (297˚) and (J_1 with J_3) in direction (310˚). While at station (2), a possibility of planar sliding on (J_2) in direction (325˚) and direct toppling as a result of the intersection of (J_1) and (J_3) in direction (304˚), with no wedge sliding or flexural toppling.

At station (3), there is a possibility of planar sliding on (J_2) in the direction (279˚), and wedge sliding in the direction (343˚) as a result of the intersection of (J_2 with J_3). No possibility of flexural and direct toppling is noticed. Whereas at station (4), the planar sliding on (J_1) in direction (111˚) is shown, as well as the possibility of the wedge sliding as a result of the intersection of (J_1 with J_2) in direction (032˚), and (J_1 with J_3) in direction (057˚); in addition to the possibility of the direct toppling occurring as a result of the intersection of (J_2 with J_3) in direction (108˚), while no possibility of a flexural toppling. At station (5), the wedge sliding results from the intersection of (J_1 with J_2) in direction (269˚), as well as the possibility of flexural toppling in direction (227˚) on (J_3), while there is no possibility of plane sliding or direct toppling. At the last station (6), the possibility of planar sliding occurred on (J_3) in direction (142˚). Wedge sliding occurs as a result of the intersection of (J_3 with J_1) in direction (221˚) and (J_3 with J_2) in direction (197˚), with no possibility of flexural or direct toppling.

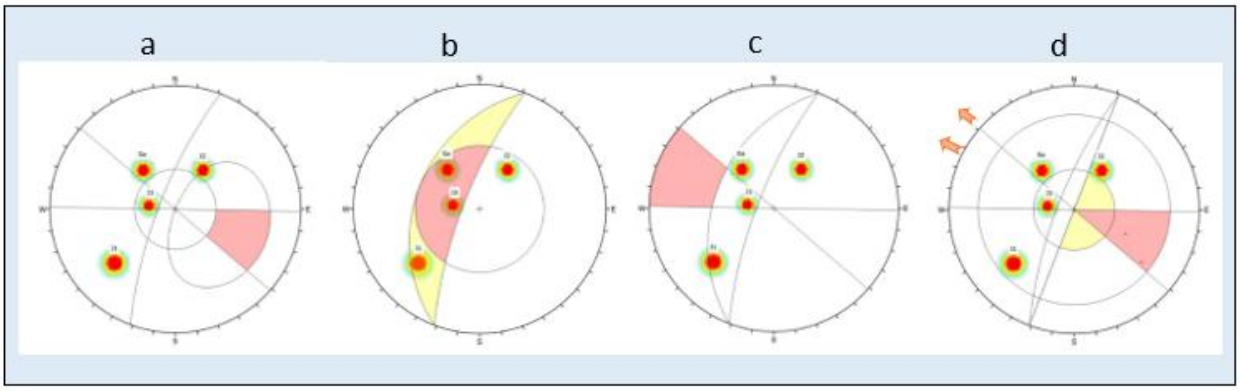

Fig. 12: Possibility of expected failures at station (1): (a) no plane sliding, (b) no wedge sliding, (c) no flexural toppling. (d) the possibility of direct toppling, where the intersection of (J_1 with S_o) appears in the direction (297°) and (J_1 with J_3) in the direction (310°).

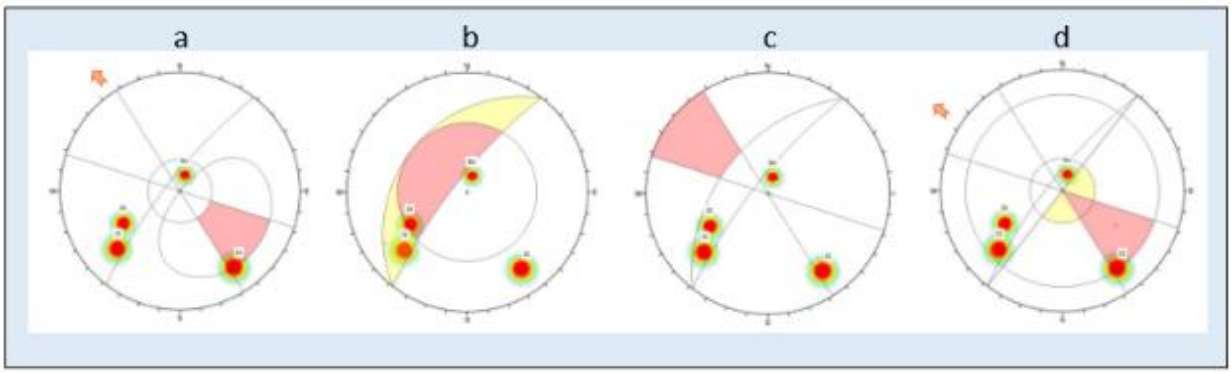

Fig. 13: Expected failure possibilities at station (2): (a) possibility of plane sliding of (J_2) in the direction of (325°), (b) no wedge sliding, (c) no flexural toppling, (d) possibility of direct toppling where the intersection of (J_1) and (J_3) appears in the direction (304°).

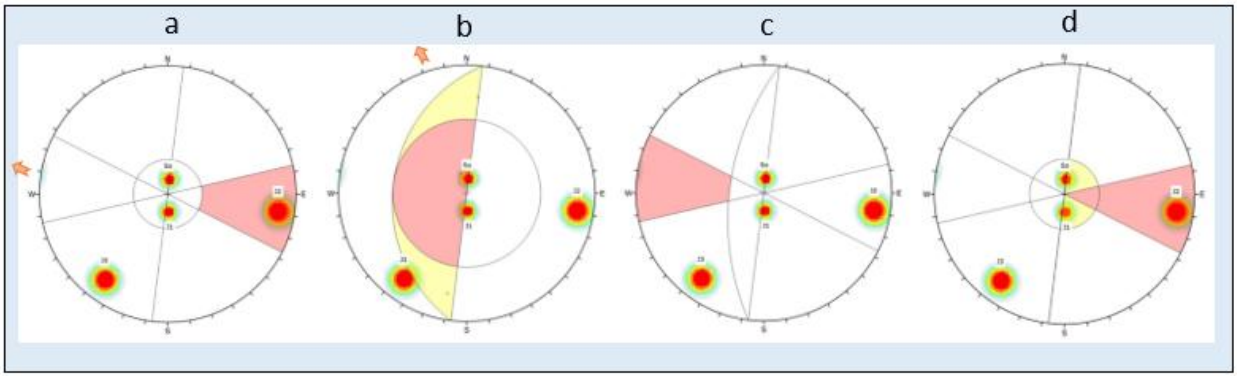

Fig. 14: Expected failure possibility at station (3): (a) possibility of planer sliding on (J_2) in the direction of (279°), (b) possibility of wedge sliding in the direction of (343°) as a result of the intersection of (J_2 with J_3), (c) no possibility of a flexural toppling, (d) no possibility of a direct toppling.

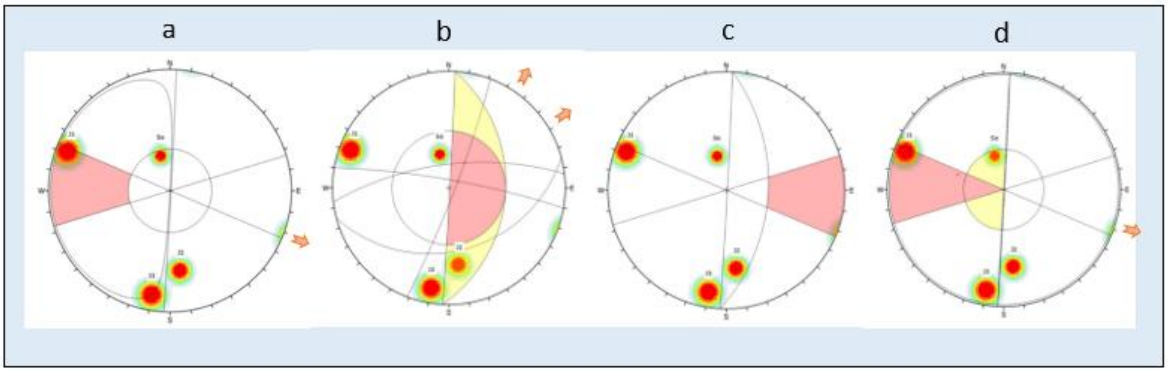

Fig. 15: Expected failure possibilities at station (4): (a) possibility of planar sliding on (J1) in the direction (111°), (b) possibility of wedge sliding resulting from the intersection of (J_1 with J_2) in the direction (032°) and (J_1 with J_3) in the direction (057°), (c) possibility of a flexural toppling, which has not been shown, (d) possibility of a direct toppling resulting from the intersection of (J_2 with J_3) in the direction (108).

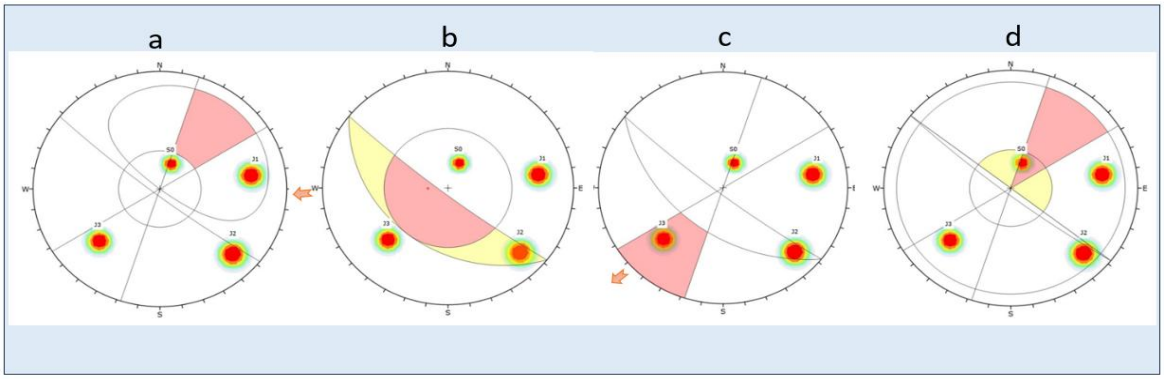

Fig. 16: Expected failure cases at station (5): (a) no possibility of plane sliding, (b) possible wedge sliding resulting from the intersection of (J_1 with J_2) in the direction (269°), (c) possible flexural toppling on (j_3) in the direction (227°), (d) no possibility of direct toppling.

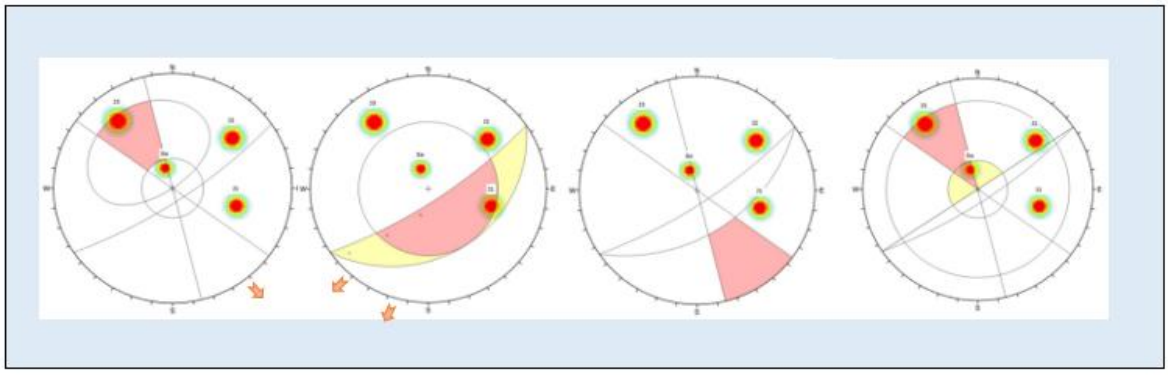

Fig. 17: Expected failure cases at station (6): (a) possibility of planar sliding on (J_3) in direction (142°), (b) possibility of wedge sliding occurring as a result of the intersection of (J_3 with J_1) in direction (221°) and the intersection of (J_3 with J_2) in direction (197°), (c) no possibility of a flexural toppling, (d) no possibility of a direct toppling.

After finding the possible failure cases in the stations, their results are entered in (SMR Tool-v205) software (with the values of (RMRb) and slope direction, and determining the discontinuity surfaces obtained by each possible failure case) (Riquelme et al., 2014) to find the values of (SMR) and classify the cases according to Romana (1985) and Romana et al. (2003) to evaluate the stability of each case and at each station. The software processes the data and finds the values of (F1), (F2), and (F3) after determining the type of slope mechanical drilling in the study area. The results are shown in Table 4.

Table 4: Results of slope stability analysis with possible failure modes at each discontinuity surface and their directions, (F1, F2, F3) values, (SMR) values with class, description, and stability.

stations	slopes	RMR_b	failures	discontinuities	direction	F_1	F_2	F_3	F4	$F_1F_2F_3$	SMR	class	description	Stability
S1	291\75	67	Direct toppling	J_1+S_o	297˚	1	1	-6	0	-6	61	II	good	stable
				J_1+J_3	310˚	0.7	1	0	0	0	67	II	good	stable
S2	308\77	75	Planner sliding	J_2	325˚	0.7	1	-50	0	-35	40	IV	bad	unstable
			Direct toppling	J_1+J_3	304	1	1	-6	0	-6	69	II	good	stable
S3	277\90	73	Planner sliding	J_2	279˚	1	1	-50	0	-50	23	IV	bad	unstable
			Wedge sliding	J_2+J_3	343˚	0.15	1	-60	0	-9	64	II	good	stable
S4	093\89	74	Planner sliding	J_1	111˚	0.7	1	-50	0	-35	39	IV	bad	unstable
			Wedge sliding	J_1+J_2	032	0.15	1	-60	0	-9	65	II	good	stable
				J_1+J_3	057	0.15	1	-60	0	-9	65	II	good	stable
			Direct toppling	J_2+J_3	108	0.7	1	-25	0	-17.5	56	III	normal	Partially stable
S5	218\84	74	Wedge sliding	J_1+J_2	269	0.15	1	-60	0	-9	65	II	good	stable
			Flexural toppling	J_3	227˚	0.85	1	-25	0	-21.25	52	III	normal	Partially stable
S6	146\77	63	Planner sliding	J_3	142˚	1	1	-50	0	-50	13	V	Very bad	Completely unstable
			Wedge sliding	J_1+J_3	221	0.15	0.7	-60	0	-6.3	56	III	normal	Partially stable
				J_2+J_3	197	0.15	1	-60	0	-9	54	III	normal	Partially stable

First, it is noted from the kinematic analysis that wedge sliding is the most likely, where it appears at stations (3, 4, 5 and 6), and it appears twice at stations (4 and 6), as the intersection of the joint surfaces helps in the occurrence of the wedge sliding. Second is plane sliding, which occurs at stations (2, 3, 4, and 6), where the joints trend the same as the slopes in some parts, and their angles of inclination are less than the angles of the slopes, so they are auxiliary surfaces for the occurrence of the plane sliding. On the other hand, the flexural toppling is the last possibility, as it is shown only at station (5).

From the final analysis of (SMR), it appears that station (1) is the most stable, which shows one failure possibility, which is a direct toppling from the intersection of J_1 with both S_o and J_3, both of which are good and stable and need only occasional reinforcement by (Bolts, Anchors). In contrast, station (6) appears to be the least stable station, at which two possible failures appear; first, is a very bad and completely unstable from planar sliding on J_3, which requires support by (Reexcavation Walls); second, is normal and partially stable from wedge sliding resulted from intersection of (J_1 with J_3) and (J_2 with J_3) that require support systematically by concrete.

4. Conclusions

The comprehensive field survey of the study area, laboratory tests, mathematical analyses, and results of the software reveal the following:

The possibility of failures at station (1) is in two cases of direct toppling, which are the intersection of the (J1) with both (So) towards (297˚), where the (SMR) value reached (61), and with (J3) towards (310˚), where the (SMR) value reached (67). Both are stable cases; the support is

occasional by (Bolts and Anchors). At Station (2), there are two possible failures appear too, plane sliding on (J2) in the direction (325) where its surface is directed in the same direction as the slope in some parts, so it became a surface that helps to sliding as the value of (SMR) is (40), which is a bad unstable case, and support is important and must be corrected by surface drainage or deep drainage. The second possible failure at station (2) is direct toppling in the direction (304˚) from the intersection of (J1 with J3) with an (SMR) value of (69), which is a good and stable case; the support is occasional by (Bolts and Anchors).

Also, two possible failures appear at station (3); the first is the plane sliding on (J2) in the direction of (279˚), where its surface is in the same direction as the slope in some parts, so it became a surface that helps to sliding. Despite the rock characteristics that show a very high (UCS), excellent (RQD), and high (ϕ), the (SMR) value is (23), so it is a bad unstable case, and support is important and must be treated by (Reexcavation Walls). The second possible failure in this station is the wedge sliding from the intersection of (J2 with J3) in the direction of (343˚) according to Markland (1972). The (SMR) value is (64), indicating a good stable case with occasional support by (Bolts and Anchors). On the other hand, there are three failure types at station (4); the first is the planer sliding on (J1) in the direction (111˚) as its surface is in the same direction as the slope in some parts, which made it a surface that helps to slide, whose (SMR) value is (39), so it is a bad unstable case, and support is important and must be corrected by (Surface drainage and Deep drainage). The second is the wedge sliding from the intersection of (J1 with J2) in the direction (032˚), and the intersection of (J1 with J3) in the direction (057˚), and in both cases the value is (65), so they are two good stable cases. The third failure is the direct toppling from the intersection (J2 with J3) in the direction (108˚), whose (SMR) is (56), which is a normal and partially stable case that requires (systematic) support by concrete.

Station (5) has two possible failures; the first is wedge sliding from the intersection of (J1 with J2) in the direction (269˚) with (SMR) value of (65); so it is a good and stable case that support occasionally, while the second is the flexural toppling on (J3) in the direction (227˚) with (SMR) value of (52); it is a normal and partially stable case that requires a systematic support by concrete.

Finally, there are also two possible failures at Station (6); the first is least stable, representing planar sliding on (J3) in the direction of (142˚) because its direction is inclined in the same direction as the slope in some parts, which makes it a surface that helps to slide. (SMR) is (13), so it is a very bad and completely unstable, which requires support by (Reexcavation Walls); while the second possible failure is wedge sliding from the intersection of (J1 with J3), which gives (SMR) value of (56), and the intersection of (J2 with J3), whose (SMR) is (54); both are normal and partially stable cases that require support systematically by concrete.

5. Acknowledgments

The authors would like to thank Dr. Saddam Al-Khatony, Dr. Jinan Barno and Mr. Saad Naef Al-Fahdawi for their assistance in completing this work. They also would like to thank Father John (responsible for Rabban Hormizd Monastery) for the facilities he provided to complete the fieldwork.

6. References

Al Sumaidaie, M.A.H., Abdullah, N.M.R., Al-Jawadi, A.S. and Alkhatony, S.E., 2024. Classification, Hazard Assessment, and Optimization Strategy for Some Critical Rockfall Locations in the Duhok Area, North of Iraq, Iraqi Geological Journal, 57 (2D), 137-146, https://doi:10.46717/igj.57.2D.11ms-2024-10-21 .

Al-Habity, S. T. A., Abood, M. R. and Aljumaily, I. S. I., 2025. Assessment of Rock Slopes Stability Located on the Banks of the Khanas Dam Reservoir in the Nineveh Governorate, Northern Iraq. Articles in Press, Accepted Manuscript, Available Online from 19 January 2025, DOI:10.33899/earth.2024.149320.1280

Al-Jawadi, A.S., 2021. Theoretical Models of Slope Stability Analysis in The Maqlub Mountain Rock Cut Routes, North Iraq, 2021, The Iraqi Geological Journal, 54 (1A), pp. 55-68, DOI: https://10.46717/igj.54.1A.6Ms-2021-01-27 .

Al-Jawadi, A.S., Al-Jumaily, I.S., Al-Dabbagh, T.H., and Davie, C., 2023. Evaluation of the Bekhme Dam Site – NE Iraq using the Proposed Reduction System of the Rock Mass Strength, Iraqi National Journal of Earth Science, 2023, 23(1), pp. 85–106, https://doi:10.33899/EARTH.2023.137501.1036 .

Anon, 1972. The preparation of Maps and Plans in Terms of Engineering Geology, Quarterly Journal of Engineering Geology, Vol.5, No.4, pp. 293-382.

Anon, 1977. The description of rock masses for engineering purposes, Report by the Geological Society Engineering Group Working Party, Quarterly Journal of Engineering Geology, Vol. 10, pp.355-388.

Bieniawski, Z. T., 1973. Engineering classification of jointed rock masses. Trans. South African Institution of Civil Engineers, Vol. 15, pp. 335-344.

Bieniawski, Z.T., 1989. Engineering Rock Mass Classification, John Wiley, New York, U.S.A.

Broch, E. and Franklin, J.A., 1972. The Point Load Strength test, International Journal of Rock Mechanics and Mining Sciences and Geomechanics Abstracts, Vol. 9, No. 6, pp. 669-697, DOI:10.1016/ 0148-9062(72)90030-7.

Bromhead, E.N., 1992. The Stability of Slopes, 2nd ed., Blackie Academic and Professional, Great Britain, CRC Press, pp.424.

Bruce, I. G., Cruden D. M. and Eaton T. M., 1989. Use of a Tilting Table to Determine the Basic Friction Angle of Hard Rock Samples. Canada Geotechnical Journal, January 2011, Vol. 26, No. 3, pp. 474-479, DOI:10.1139/t89-060.

Clague, J.J. and Steed, D., 2012. Landslides: Types, Mechanisms, and Modeling. PP. 436, Cambridge University Press.

Deere, D.U., Hendron, A.J., Patton, F.D. and Cording, E.J., 1966. Design of surface and near surface construction in rock. Paper presented at the 8th U.S. Symposium on Rock Mechanics (USRMS), pp. 66-0237.

Duncan, J. M., 2000. Factors of Safety in Geotechnical Engineering. Journal of Geotechnical and Geoenvironmental Engineering, Vol. 126, No. 4, DOI:10.1061/(ASCE)1090-0241(2000)126:4(307).

Fell, R., MacGregor, P., Stapledon, D., Bell, G. and Foster, M., 2014. Geotechnical engineering of dams (2nd ed.). CRC Press, p. 1382, DOI:10.1201/b17800.

Gunsallus, K.L. and Kulhawy, F.H., 1984. A comparative Evaluation of Rock Strength Measures, International Journal of Rock Mechanics and Mining Sciences and Geomechanics Abstracts. Vol. 21, No.5, pp. 233-248, DOI:10.1016/ 0148-9062(84)92680-9.

Hoek, E. and Bray, J.W., 1981. Rock Slope Engineering, 3rd ed., Institution of Mining and Metallurgy, London, 358 P.

ISRM, 1985. Suggested method for determining point load strength, Inst. J. Rock Mech. Min. Sci. Vol. 22, pp. 51-60.

Iverson, R. M., 2000. Landslide triggering by rain infiltration. Water Resources Research, Vol.36, No.7, 1897-1910, DOI:10.1029/2000WR900090.

Jassim S.Z. and Goff J.C., 2006. Geology of Iraq. DOLIN, S.R.O., distributed by Geological Society of London, pp. 341.

Kohno, M. and Maeda, H., 2018. Correlations Between Point Load Strength Index and Physical Properties of Hydrothermally Altered Rocks. International Journal of Engineering and Mineral Processing, Vol. 7, No. 1, pp. 1-13. DOI: 10.5923/j.mining.20180701.01.

Markland, J. T. 1972. A useful technique for estimating the stability of rock slopes when the rigid wedge slide type of failure is expected, Interdepartmental Rock Mechanics Project, Imperial College of Science, pp 10-26.

Palmström, A., 1982. The volumetric joint count: a useful and simple measure of the degree of rock jointing. Proc. 4th congr. Int. Assn Engng Geol., New Delhi 5, 221-228.

Pantelidis, L., 2009. Rock Slope Stability Assessment Through Rock Mass Classification Systems, International Journal of Rock Mechanics and Mining Sciences, Vol. 46, No. 2. pp. 315-325, DOI: 10.1016/ j. ijrmms.2008.06.003.

Riquelme, A., Abellán, A.,Tomás, R., 2014. SMRTool beta. A calculator for determining slope mass rating (SMR). Universidad de Alicante.

Rocscience Inc. Dip v. 6.008 software 2015. Rocscience, Toronto, Canada.

Romana, M., 1985. New Adjustment ratings for Application of Bieniawski Classification to Slopes, Proceedings of the International Symposium on the Role of Rock Mechanics in Excavations for Mining and Civil Works. International Society of Rock Mechanics, Zacatecas, pp. 49-53.

Romana, M., Serón, J.B. and Montalar, E., 2003. "SMR Geomechanics Classification: Application, Experience and Validation", Proceedings of the 10th Congress of the International Society for Rock Mechanics, South Africa, Sandton, South Africa, September.

Romana, M., Tomas R. and Seroon J. B., 2015. Slope mass rating (SMR) Geomechanics classification: Thirty years review, 13th ISRM International Congress of Rock Mechanics. International Society for Rock Mechanics and Engineering.

Romana, M.R. 1993. A Geomechanical Classification for Slopes: Slope Mass Rating, Pergamon Press, Oxford, New York, Vol. 3, pp. 575-600. DOI:10.1016/B978-0-08-042066-0.50029-X.

Rowe, R. K. (Ed.), 2001. Geotechnical and Geoenvironmental Engineering Handbook. Springer US, pp. 1625.

Rusnak, J. and Mark C., 2000. Using The Point Load Test to Determine the Uniaxial Compressive Strength of Course-Measured Rock. Proceedings of 19th international conference on ground control in mining, Morgantown, WV, pp. 362-371.

Salunkhe, D.P., Chvan G., Bartakke R. N. and Kothavale P. R., 2017. An Overview on Methods for Slope Stability Analysis. International Journal of Research and Technology, Vol. 6, No. 03.pp. 528-535, DOI: 10.17577/IJERTV6IS030496.

Sissakian, V. K., Jabbo B. R., Al-Ansari N. and Knutsson S., 2016. Age Estimation of Alqosh Main Landslide, North Iraq Using Exposure Dating Method, Journal of Earth Sciences and Geotechnical Engineering, Vol.6, No. 3, pp. 163-176.

Ullah, S., Khan M. U. and Rehman G., 2020. A brief Review of The Slope Stability Analysis Methods, Geological Behavior (GBR), Vol. 4, No. 2, pp. 73-77, DOI: DOI:10.26480/gbr.02.2020.73.77.

Iraqi National Journal of Earth Science, Vol. 26, No. 03, 2026 (237-252)

Iraqi National Journal of Earth Science

www.earth.uomosul.edu.iq

تحليل استقرار المنحدرات الصخرية على طريق دير (الربان هرمزد) في طية ألقوش المحدبة، شمالي العراق

نوال محمد على ال عبدالله [1*]، محمد راشد عبود [2]، عمار جماد محمد [3]

nawal.muhammad@st.tu.edu.iq mrabood@tu.edu.iq geoamaar1977@edu.tu.iq

[1] مديرية تربية نينوى، نينوى، العراق.

[2] قسم علوم الأرض التطبيقية، كلية العلوم، جامعة تكريت، تكريت، العراق.

[3] قسم علوم الأرض التطبيقية، كلية العلوم، جامعة تكريت، تكريت، العراق.

تاريخ الاستلام: 24 اذار 2025 تاريخ المراجعة: 06 ايار 2025 تاريخ القبول: 09 حزيران 2025

تاريخ النشر الالكتروني: 01 تموز 2026

الملخص

تشمل أهداف الدراسة الحالية تحليل استقرارية المنحدرات الذي تم إجراؤه عن طريق التحليل الحركي وتصنيف كتلة المنحدر (SMR) في ست محطات مختارة على طريق دير (الربان هرمز) الواقع في طية القوش المحدبة، شمالي العراق. تُظهر الدراسة الحالية أن المحطة (1) فيها احتمالان لحدوث الانقلاب المباشر من تقاطع (J1) مع كل من مستوى التطبق (S0) و(J3)، وكلاهما حالتان مستقرتان. تُظهر المحطة (2) حالتين محتملتين، الأولى هي الانزلاق المستوي على (J2)، وهي حالة سيئة وغير مستقرة. أما الحالة الثانية فهي الانقلاب المباشر من تقاطع (J1) مع (J3)، وهي حالة جيدة ومستقرة. تُظهر المحطة (3) حالتين محتملتين، الأولى هي (J2) بقيمة (SMR) مساوية (23)، لذا فهي حالة سيئة وغير مستقرة. أما الثانية فهي الانزلاق الإسفيني من تقاطع (J2) مع (J3)، وهي حالة جيدة ومستقرة. في المحطة (4)، ظهرت ثلاث حالات انهيار محتملة. الأولى هي الانزلاق المستوي على (J1)، وهي حالة سيئة وغير مستقرة. أما الحالة الثانية فهي الانزلاق الإسفيني من تقاطع (J1) مع كل من (J2) و(J3)، وفي كلتا الحالتين قيمة (SMR) تساوي (65)، لذا فهما حالتان جيدتان ومستقرتان. الحالة الثالثة المحتملة هي الانقلاب المباشر من تقاطع (J2 مع J3)، وهي حالة طبيعية ومستقرة جزئيًا. تُظهر المحطة (5) حالتين، الأولى هي الانزلاق الإسفيني من تقاطع (J1 مع J2)، وهي حالة جيدة ومستقرة؛ والثانية هي الانقلاب الانثنائي على (J3)، وهي حالة طبيعية ومستقرة جزئيًا. تُظهر المحطة (6) حالتين، الأولى هي الانزلاق المستوي على (J3) بقيمة (SMR) تساوي (13)، وهي حالة سيئة للغاية وغير مستقرة تمامًا، وتتطلب دعمًا بواسطة (جدران إعادة الحفر)؛ أما الحالة الثانية المحتملة فهي الانزلاق الإسفيني من تقاطع (J3) مع كل من (J1 و J2)، وكلاهما حالتان طبيعيتان ومستقرتان جزئيًا.

الكلمات المفتاحية:

الربان هرمزد، التحليل الحركي، أنواع الدعم

DOI: 10.33899/injes.v26i3.60933, ©Authors, 2026, College of Science, University of Mosul.

==========